Sains Malaysiana 54(1)(2025): 211-224
*http://doi.org/10.17576/jsm-2025-5401-17*

# Enhanced Toxicity and Antifungal Effects of Iron-Oxide Chitosan/Samarium/ Ranitidine Microparticles

(Ketoksikan Dipertingkatkan dan Kesan Antikulat bagi Zarah Mikro Kitosan/Samarium/Ranitidine Oksida Besi)

ENY KUSRINI[1,2,3,*], KHAIRU NUZULA[1], ANWAR USMAN[4], LEE D. WILSON[5], CINDY GUNAWAN[6] & AGUS BUDI PRASETYO[7]

[1]*Department of Chemical Engineering, Faculty of Engineering, Universitas Indonesia, Kampus Baru UI Depok, 16424, Indonesia*
[2]*Research Group of Green Product and Fine Chemical Engineering, Laboratory of Chemical Product Engineering, Department of Chemical Engineering, Universitas Indonesia, Kampus Baru UI, Depok, 16424, Indonesia*
[3]*Tropical Renewable Energy Research Center, Faculty of Engineering, Universitas Indonesia, Kampus Baru UI, Depok, 16424, Indonesia*
[4]*Department of Chemistry, Faculty of Science, Universiti Brunei Darussalam, Jalan Tungku Link, Gadong BE1410, Negara Brunei Darussalam*
[5]*Department of Chemistry, University of Saskatchewan 110 Science Place, Room 156 Thorvaldson Building, Saskatoon, SK S7N 5C9, Canada*
[6]*ithree institute, University of Technology Sydney, Sydney, NSW 2007, Australia*
[7]*Research Center for Metallurgy, National Research and Innovation Agency (BRIN), KST, BJ. Habibie, Puspitek Area, Setu, Tangerang Selatan, 15314, Indonesia*

*Received: 25 June 2024/Accepted: 30 October 2024*

ABSTRACT

This study aimed to investigate the cytotoxicity and antifungal properties of $Sm(NO_3)_3.6H_2O$ salt, chitosan/Sm complex, iron oxide ($Fe_3O_4$ NPs), and iron-oxide modified chitosan/Sm/ranitidine microparticles. The microparticles of iron-oxide modified chitosan/Sm/ranitidine composites were synthesized from various masses of $Sm(NO_3)_3.6H_2O$ (250-350 mg), chitosan (2,000-2,500 mg), and (5-25 mg) through the microwave-assisted evaporation method. The $Fe_3O_4$ NPs and ranitidine/Sm were mixed with chitosan through a dispersion method by microwave. The toxicity studies of iron-oxide modified chitosan/Sm/ranitidine composites showed 50% lethal concentration in the range from 3,600 to 3,900 µg/mL on the aquatic crustacean *Artemia salina*, suggesting their slight toxicity. Antifungal activities for all samples were determined using the agar diffusion and serial dilution methods. The iron-oxide modified chitosan/Sm/ranitidine composites showed inhibition zone diameter of *Aspergillus niger* from 18.33 to 14.67 mm at 1,000 µg/mL. All composites and chitosan/Sm complex showed bioactivity properties with minimum inhibitory concentration values of 2.5 µg/mL against *A. niger*. These composites and chitosan/Sm complex have the same minimum fungicidal concentration, showing the potential to inhibit fungi. Overall results suggested that modifying the structure of chitosan using $Sm^{3+}$, $Fe_3O_4$ NPs, and ranitidine enhanced its physical, chemical, and biological properties as an antifungal agent.

Keywords: Antifungal agent; cytotoxicity studies; iron-oxide modified chitosan/Sm/ranitidine microparticles; microwave-assisted evaporation

ABSTRAK

Penyelidikan ini bertujuan untuk mengkaji sifat ketoksikan dan antikulat garam $Sm(NO_3)_3.6H_2O$, kompleks kitosan/ Sm, oksida besi ($Fe_3O_4$ NPs) dan zarah mikro kitosan/Sm/ranitidin terubah suai besi-oksida. Zarah mikro bagi komposit kitosan/Sm/ranitidine terubah suai besi-oksida telah disintesis daripada pelbagai jisim $Sm(NO_3)_3.6H_2O$ (250-350 mg), kitosan (2,000-2,500 mg) dan (5-25 mg) melalui kaedah penyejatan gelombang mikro-berbantu. NP $Fe_3O_4$ dan ranitidine/ Sm dicampur dengan kitosan melalui kaedah serakan oleh gelombang mikro. Kajian sitotoksisiti bagi komposit kitosan/ Sm/ranitidine terubah suai besi-oksida menunjukkan 50% kepekatan maut dalam julat dari 3,600 hingga 3,900 µg/mL pada krustasea akuatik *Artemia salina* yang menunjukkan sedikit ketoksikannya. Aktiviti antikulat untuk semua sampel ditentukan menggunakan kaedah penyebaran agar dan pencairan bersiri. Komposit kitosan/Sm/ranitidine terubah suai besi-oksida menunjukkan diameter zon perencatan *Aspergillus niger* daripada 18.33 hingga 14.67 mm pada 1,000 µg/mL. Semua komposit dan kompleks kitosan/Sm menunjukkan sifat bioaktiviti dengan nilai kepekatan perencatan minimum 2.5 µg/mL terhadap *A. niger.* Komposit dan kompleks kitosan/Sm ini mempunyai kepekatan racun kulat minimum yang sama yang

menunjukkan potensi untuk menghalang kulat. Keputusan keseluruhan mencadangkan pengubahsuaian struktur kitosan menggunakan $Sm^{3+}$, $Fe_3O_4$ NPs dan ranitidine meningkatkan sifat fizikal, kimia dan biologinya sebagai agen antikulat.

Kata kunci: Agen antikulat; kajian ketoksikan; mikro zarah kitosan/Sm/ranitidine terubah suai besi-oksida; penyejatan gelombang mikro-berbantu

## INTRODUCTION

Rare earth element (REEs) is widely recognized as lanthanides, comprising 17 elements, are widely recognized as lanthanides, which are critical minerals (Kusrini et al. 2024). The lanthanide complexes have been reported and applied as antifungal, antibacterial, and antioxidant agents (Chandra & Agrawal 2014; Cota, Marturano & Tylkowski 2019; Devineni et al. 2013; Mohanan, Kumari & Rijulal 2008; Momani et al. 2012; Patil et al. 2011; Rahdar et al. 2019). In addition, Cerium(III) picrate tetraethylene glycol complex is recently reported as anti-amoebic agent against *Acanthamoeba* sp. (Kusrini et al. 2020). Due to their efficient bioactivities, samarium-chitosan composites have also gained significant attention in biomedical applications such as in drug delivery system (Kusrini et al. 2014). The samarium- chitosan composites have excellent fluorescence properties as well as active functional groups, allowing them to be used as an indicator of drug release, for example ibuprofen (IBU) as a model drug.

The effect of additional $Sm^{3+}$ ions on chitosan (especially for chitosan–Sm 25 wt.%) makes the composites able to adsorb the IBU drug with an adsorption efficiency as high as 33.04% (Kusrini et al. 2014). On the other hand, a design of antimicrobial active agent using dysprosium nanoparticles coated on contact lenses as carrier against *Acanthamoeba* keratitis has also been reported by Kusrini et al. (2021). From these previous studies, REEs are used to enhance the biological activities and increase their capability as drug delivery and/or their antimicrobial activities. Investigation and analysis of application of REE that incorporated with magnetite nanoparticles ($Fe_3O_4$ NPs) as a drug carrier have also reported. It was reported that the luminescence and magnetic properties of REE-magnetite NPs allowed for easy tracking based on luminescence character of REEs and more easy separation because of the presence of $Fe_3O_4$ NPs (Peng et al. 2012; Wang, Xiangpeng & Kezheng 2011; Zhao, Qiu & Huang 2008).

Chitosan considered as a safe and effective drug delivery system due to its biocompatibility, biodegradability, and physicochemical properties (Asrahwi et al. 2023; Kusrini et al. 2014; Patel, Patel & Patel 2010; Rosman et al. 2023; Usman et al. 2024). Although it has antifungal properties, chitosan can only dissolve in a slight acidic condition (Qin, Lia & Guo 2020). In this study, the iron-oxide modified chitosan/Sm/ranitidine composites were synthesized by the microwave-assisted evaporation method. Microparticles composite based on the iron-oxide modified chitosan/Sm/ranitidine were designed and synthesized for drug delivery systems with ranitidine as a drug model. Ranitidine is known as a drug to cure infection in gastrointestinal tract and can be degraded by enzymes in acidic conditions. To deliver drug into gastrointestinal tract, the drug will be encapsulated by chitosan in composites. The complexation includes the use of ranitidine to treat stomach infection, $Sm^{3+}$ ion with luminescence properties for drug delivery tracking, and $Fe_3O_4$ to facilitate drug carrier separation.

The limitation of chitosan as matrix in drug carrier is that it cannot be used to monitor the release of drug without any additional marker or material containing luminescence such as lanthanides. Thus, the challenge to design a new drug carrier is to have a host that can be tracked as well as to accommodate load of drug that can be monitored, and its release can be adjusted. With this idea, we design a structure of cationic chitosan as a matrix in the drug carrier by adding an active agent, such as lanthanide, magnetite, and other components. This modification is carried out to improve the solubility, performance in a wide pH range, and antifungal properties (Qin, Lia & Guo 2020; Wibowo et al. 2021). The design of drugs, composites, and active compounds using lanthanides has a significant impact on the medical sector. Therefore, further investigation related to lanthanides and their composites for medical applications is essential to obtain the highest standards of living, health, and welfare.

The iron-oxide modified chitosan/Sm/ranitidine composites was synthesized using the microwave-assisted evaporation method. Four different compositions of composites denoted as composites A, B, and C, were synthesized based on chitosan, Sm, $Fe_3O_4$, and ranitidine with different contents; i.e., samarium salt (250 - 350 mg), chitosan (2,000 - 2,500 mg) and $Fe_3O_4$ NPs (5 - 25 mg), respectively. Composite A is comprised of four ingredients with a composition of ranitidine (100 mg), $Fe_3O_4$ NPs (5 mg), chitosan (2,000 mg), and $Sm(NO_3)_3.6H_2O$ (350 mg). Composite B contained ranitidine (100 mg), $Fe_3O_4$ NPs (5 mg), chitosan (2,500 mg) and $Sm(NO_3)_3.6H_2O$ (250 mg). Meanwhile, composite C comprised four ingredients with a composition of ranitidine (100 mg), $Fe_3O_4$ NPs (25 mg), chitosan (2,000 mg), and $Sm(NO_3)_3.6H_2O$ (250 mg). All composites were tested against *Aspergillus niger* using two different methods, namely the agar diffusion and serial dilution tests. The expected output from this study is to obtain the optimum iron-oxide modified chitosan/Sm/ranitidine composite that possess the highest inhibition zone diameter and has strong antifungal activities.

## EXPERIMENTAL DETAILS

### MATERIALS

Dimethylformamide (DMF) and acetic acid were purchased from Merck (Germany). Dimethyl sulfoxide (DMSO), iron(II) chloride tetrahydrate ($FeCl_2.4H_2O$), iron(III) chloride hexahydrate ($FeCl_3.6H_2O$), and samarium(III) nitrate hexahydrate ($Sm(NO_3).6H_2O$) were purchased from Sigma Aldrich (Wisconsin, USA). A medical grade chitosan powder with deacetylation degree of 90.77%, off-white, viscosity of 18 cps, moisture content of 6.61%, ash content of 0.73%, protein content of 60.5%, and pH 7-8 was purchased from PT Biotech Surindo (Cirebon, Indonesia). *A. niger* was provided by Indonesia Institute of Science (LIPI, Indonesia), while potato dextrose agar (PDA) media was purchased from Himedia Laboratories Ltd. (Indonesia). Methanol and sodium tripolyphosphate (TPP) were purchased from PT. Brataco (Indonesia). Moreover, reagents such as ammonium hydroxide ($NH_4OH$), acetic acid ($HC_3COOH$), ultrapure water, PDA, and TPP were used without any purification.

### PREPARATION OF THE IRON OXIDE NANOPARTICLES

The iron oxide ($Fe_3O_4$ NPs) was prepared using the co-precipitation method. Initially, 50 mL of 0.12 M $FeCl_2.4H_2O$ solution and 50 mL of 0.12 M $FeCl_3.6H_2O$ solution were mixed and stirred for 15 min. The mixture was added into 1 M $NH_4OH$ until pH 11, followed by stirring for 30 min and filtered using a vacuum filter. The precipitated solid was obtained, washed until pH 7, and dried in an oven at 70 °C for 4 h. Subsequently, $Fe_3O_4$ NPs were obtained and kept in a sealed bottle for further use and characterization.

### PREPARATION OF CHITOSAN/SM COMPLEX

Chitosan/Sm complex was prepared by mixing 5 mg of $Sm(NO_3)_3.6H_2O$ and 5 g of chitosan in 100 mL of distilled water with stirring using a speed of 500 rpm for 5 h. The mixture was filtered using vacuum filtration and the precipitated solid was dried in oven at 60 °C for 6 h. Chitosan/Sm complex obtained was ground and sieved for further use and characterization.

### PREPARATION OF THE IRON-OXIDE MODIFIED CHITOSAN/Sm/RANITIDINE COMPOSITES

Synthesis of the iron-oxide modified chitosan/Sm/ranitidine composites were carried out by microwave-assisted evaporation according to the method reported by Kusrini et al. (2017) with slight modifications. This method showed similarity with one-step synthesis for antimicrobial activity of silver sulfide quantum dots functionalized with highly conjugated Schiff bases reported by Shahri et al. (2022). Initially, $Fe_3O_4$ NPs were mixed with Sm nitrate, $Fe_3O_4$/Sm were coated with chitosan, and ranitidine was encapsulated using TPP as a gelation agent. The weight of $Sm(NO_3)_3.6H_2O$ salt and chitosan varied between 250-350 mg and 2,000-2,500 mg, respectively. All compositions of chitosan/Sm/$Fe_3O_4$ composites containing ranitidine are summarized in Table 1.

For composite A, 350 mg of $Sm(NO_3)_3.6H_2O$, 100 mg of ranitidine, and 5 mg of $Fe_3O_4$ NPs were mixed with 2 g of chitosan in 50 mL acetic acid solution. The suspension was mixed under stirring for 30 min, followed by microwave treatment at medium power for 15 min. Subsequently, TPP solution (100 mL) was mixed with the suspension under stirring at 500 rpm for 15 min. The precipitate was filtered using vacuum filtration and dried in an oven at 70 °C for 6 h. For composites B and C, similar procedures were applied, while the compositions of $Sm(NO_3)_3.6H_2O$, $Fe_3O_4$ NPs, and chitosan were varied. As a control, composite was also made using 100 mg of ranitidine, 5 mg of $Fe_3O_4$, 2 g of chitosan, and 250 mg of $Sm(NO_3)_3.6H_2O$ by the same method. TPP is used as a cross-linking agent (Hassani et al., 2015). The iron-oxide modified chitosan/Sm/ranitidine composites were synthesized by the microwave-assisted evaporation method, as shown in Figure 1.

### CHARACTERIZATIONS

Fourier transform infrared spectroscopy (FTIR) was used to determine functional groups of chitosan and their composites. The FTIR spectra were recorded in the range from 450 to 4000 $cm^{-1}$. The crystalline structure of composites was determined using X-ray diffraction (XRD, Pw1710) operating at 30 mA and 40 kV. Diffraction pattern was measured at 2θ angle of 10° to 89.99° with an angle

TABLE 1. Different compositions of chitosan, Sm, and $Fe_3O_4$ in composites A, B, and C

| Composites | A (mg) | B (mg) | C (mg) | Control |
|---|---|---|---|---|
| Ranitidine | 100 | 100 | 100 | 100 |
| $Fe_3O_4$ NPs | 5 | 5 | 25 | 5 |
| Chitosan | 2,000 | 2,500 | 2,000 | 2,000 |
| $Sm(NO_3)_3.6H_2O$ | 350 | 250 | 250 | 250 |

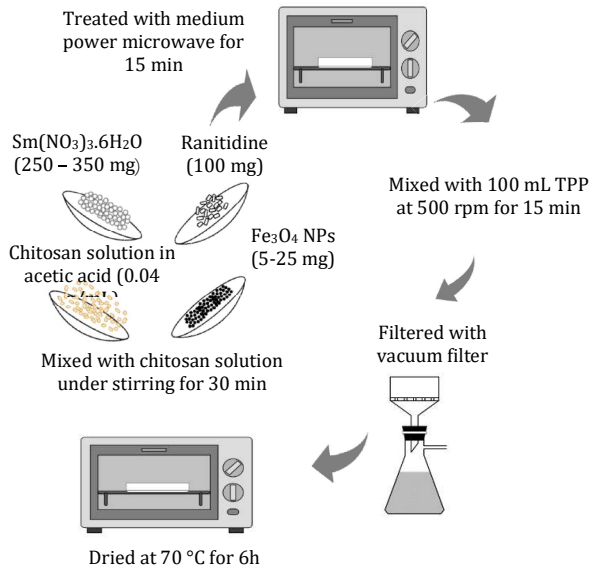


FIGURE 1. Schematic illustration for the preparation of the iron-oxide modified chitosan/Sm/ranitidine composites by microwave-assisted evaporation method

shift of 0.02°. Toxicity of composites was determined using brine shrimp lethality test (BSLT) with *A. salina* as the microorganism model. Subsequently, antifungal activity was determined using agar diffusion and serial dilution tests with *A. niger* strains as a model.

### HATCHING OF LARVAE

Sea water was inserted into an artificial hatching chamber, which was divided into two parts. One part was illuminated by light and the other was covered by cardboard, practically under dark conditions. Furthermore, 2 teaspoons of *A. salina* shrimp eggs were added into an artificial hatching chamber and air circulation was provided with an aerator for 24 h until the eggs hatched. Subsequently, the hatched eggs were kept for 24 h until maturation of larvae to juvenile phase in a fixed aerated hatching chamber.

### TOXICITY ACTIVITIES

Toxicity studies were conducted to observe the lethal dose of chitosan/Sm/$Fe_3O_4$/ranitidine composites, chitosan, $Sm(NO_3)_3.6H_2O$ salt and $Fe_3O_4$ NPs. DMSO was used both as a control and a solvent because it is non-toxic. These composites were not water-soluble, thus DMSO is used as solvent.

The cytotoxicity properties of composites were evaluated using the BLST method with *A. salina* as a model for body cells (Mayer et al. 1982). All samples (composites A, B, and C, control, samarium salt, chitosan in acetic acid solution, $Fe_3O_4$ NPs, and chitosan/Sm complex) were tested as an antifungal agent. Initially, 10 mg of each sample was dissolved in 10 mL DMSO to form a concentration of 1,000 µg/mL. The solution was sequentially diluted to obtain the concentration of 10 µg/mL, which was mixed with 5 mL of seawater and 10 mg shrimp. Sampling was carried out three times to reduce the error rate and all procedures were repeated with respect to DMSO solution without sample as a control treatment. Samples were kept under lighting for one day, followed by the observation and recording of dead larvae. All samples were prepared in concentrations of 1,000, 100, and 10 µg/mL. Toxicity analysis was determined using the BSLT method and the percentage of larvae mortality was calculated using Equation (1).

$$\%Mortality = \frac{Number\ of\ test\ deaths - number\ of\ control\ deaths}{Total\ number\ of\ larvae\ used} \times 100\% \quad (1)$$

The percentage of death concentration for each log was formed into a linear graphic. Moreover, the $LC_{50}$ value, representing 50% mortality, was determined using the linear regression method.

### ANTIFUNGAL ACTIVITY USING AGAR DIFFUSION TEST

#### PREPARATION OF CULTURE MEDIUM

The culture medium was prepared by mixing 17.9 g of PDA with 540 mL ultrapure water. A petri dish and medium were sterilized using an autoclave. After sterilization, 20 mL of the medium was added to each petri dish and kept for 2 h to solidify. PDA is a type of agar commonly used for the cultivation of fungi and bacteria.

### PREPARATION OF SAMPLES

A total of 10 mg for each composites A, B, and C, control, chitosan/Sm complex, chitosan solution, Sm salt, and $Fe_3O_4$ NPs was dissolved into 10 mL DMSO to form samples with a concentration of 1,000 µg/mL. Subsequently, 1 mL of each solution was sequentially diluted with ultrapure water to obtain the concentration of 100 µg/mL and 10 µg/mL. Similar method was conducted for Nystatin as a standard antifungal drug for comparison with each precursor. Agar diffusion method was carried out by preparing samples with different concentrations from 10 to 1,000 µg/mL and diffusing 0.1 mL into Whatman paper disc with a diameter of 10 mm.

### PROCESS OF CULTURE INOCULATION

*A. niger* culture was inoculated from the parent culture by heating the ose needle with spiritus until it turned bright red. The needle was smeared into the parent culture and immediately streaked into the culture. After each streaking, Petri dish was rotated at an angle of 60° and Whatman filter paper (10 mm) was placed in three different points on the Petri dish surface, followed by incubation for 3 days. The zone of inhibition diameter area of fungi was measured using a ruler after 3 days.

## ANTIFUNGAL ACTIVITY USING SERIAL DILUTION METHOD

### PREPARATION OF CULTURE MEDIUM

A total of 23.7 g of PDA medium was mixed with 720 mL ultrapure water. Subsequently, 20 mL of medium was poured into petri dish and sterilized with autoclaves. This was followed by pipetting 1 mL of sample into petri dish, which was individually labelled for each sample, and left for 2 h until hardened.

### PREPARATION OF SAMPLES

A total of 10 mg of each sample, including the iron-oxide modified chitosan/Sm/ranitidine composites, control, chitosan/Sm, chitosan, Sm salt, $Fe_3O_4$ NP, and Nystatin as antifungal drug control was dissolved into 1,000 mL DMSO to form a concentration of 10 µg/mL. From each sample, 5 mL was added to distilled water until the volume was 10 mL to form a solution of 5 µg/mL, and was further diluted to obtain 2.5 and 1.25 µg/mL concentrations.

### PROCESS OF CULTURE INOCULATION

*A. niger* culture was inoculated from the parent culture by heating the needle ose (loop needle) with spiritus until it turned bright red. The needle ose was smeared into the parent culture and immediately streaked into the medium when turning the petri dish at 60°. The petri dish was kept in the incubation room for 24 h and microbial growth inhibition was observed in the range of concentration from 1.25 to 10 µg/mL for all samples.

## RESULTS AND DISCUSSION

### FTIR STUDIES

The FTIR spectra of chitosan, chitosan-samarium, ranitidine, and their composites in the range of 400–4000 $cm^{-1}$ are shown in Figure S1(a)-S1(d). The vibrational bands of OH, C-H, N-H, and C-N groups of chitosan were observed at 3404, 2903, 1603, 1361, and 1032 $cm^{-1}$, while those of chitosan/Sm complex was at 3392, 2897, 1659, 1597, 1357, and 1034 $cm^{-1}$, respectively. The spectral shifts were caused by the complexation between chitosan and $Sm^{3+}$, where frequencies of the vibrational bands decreased after complexation. In chitosan/Sm complex, $Sm^{3+}$ ions were bound to hydroxyl and amine groups of chitosan (Kusrini et al. 2014). The peak at 2814 $cm^{-1}$ was attributed to C-H vibration originating from the cyclic groups of ranitidine. However, this peak was not observed in FTIR spectrum of the iron-oxide modified chitosan/Sm/ranitidine composite. Amino group of chitosan was observed at 1597 $cm^{-1}$, while the band at 1325 $cm^{-1}$ was interpreted as Fe-O bond of the iron oxide nanoparticle ($Fe_3O_4$ NPs). From FTIR spectra, ranitidine and $Sm^{3+}$ ions were successfully coordinated and formed a complex. Fe-O bond was also observed, evidencing that $Fe_3O_4$ NPs were incorporated into the iron-oxide modified chitosan/Sm/ranitidine composites, as presented in Figure 2. In this study, both the hydroxyl and amine groups from chitosan readily interacted with ranitidine.

To synthesize the microparticles composite based on the iron-oxide modified chitosan/Sm/ranitidine, lanthanide was prepared by interacting $Sm^{3+}$ ions with ranitidine, which acted as a ligand. $Fe_3O_4$ NPs and ranitidine/Sm interacted with chitosan to form composites using microwave evaporation method. This was because microwave could initiate the occurrence of chitosan cross-linking to form a hydrogel. In composites A-C, chitosan produced a cross-linking and formed a large hydrogel polymer, which allowed the absorption of $Fe_3O_4$ NPs and ranitidine/Sm onto chitosan surface. As a natural polymer, chitosan interacts with $Sm^{3+}$ ions, $Fe_3O_4$ NPs, and ranitidine through amine and hydroxyl groups on its surfaces. This interaction forms a complex and composite for further applications in industrial and medical fields.

### XRD STUDIES

In this study, XRD analysis was only performed for the iron-oxide modified chitosan/Sm/ranitidine composite. Figure 3 shows the XRD pattern of chitosan/Sm/$Fe_3O_4$/ranitidine composites, with diffraction peaks being observed at 26.8, 35.19, 39.3, 46.55, 52.29, 56.11, and 61.10°. This pattern correlated with $Fe_3O_4$ NPs (JCPDS 19-0629), which appeared at 30.5, 35.52, 43.14, 53.58, 58.02, and 62.38°.

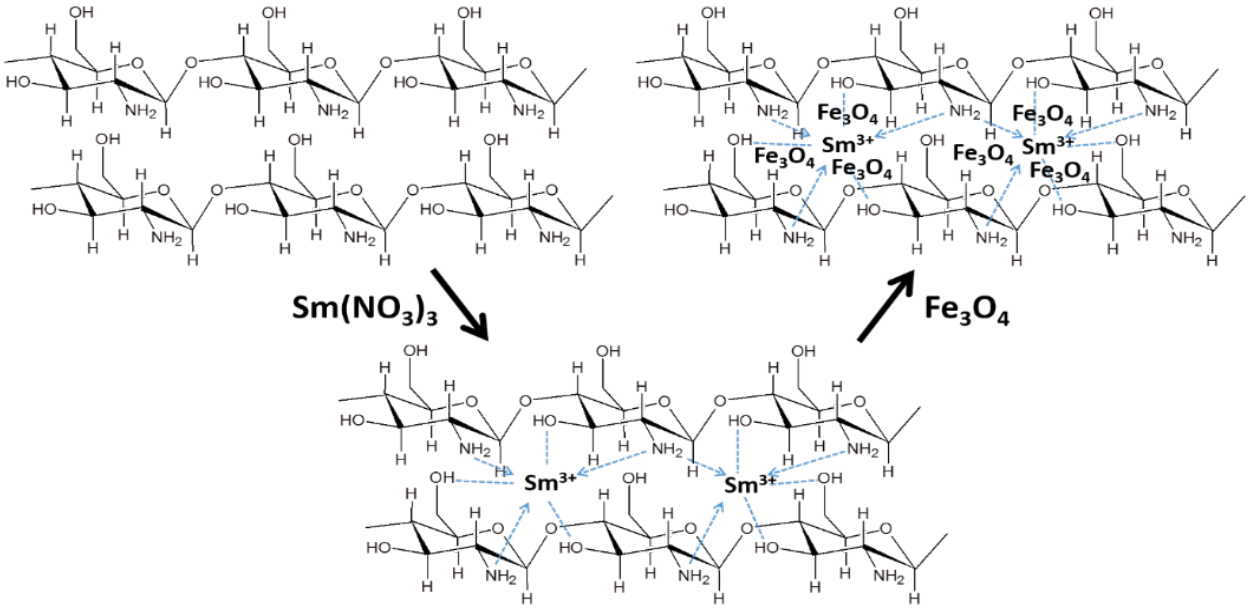


FIGURE 2. Scheme illustration for interaction between chitosan, $Sm(NO_3)_3.6H_2O$ salt, and iron oxide in the iron-oxide modified chitosan/Sm/ranitidine composites

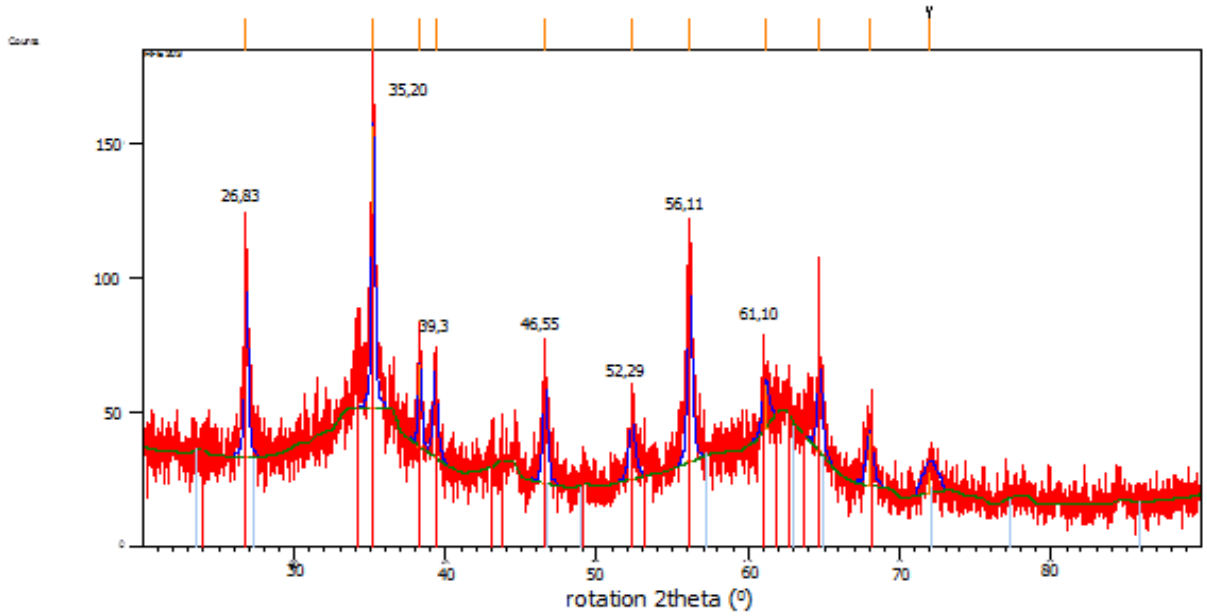


FIGURE 3. XRD pattern of the iron-oxide modified chitosan/Sm/ ranitidine composites

The peak at 18.5° showed the presence of chitosan, while a semi-crystalline structure was observed at 20° (Kusrini et al. 2013). Based on the results, the iron oxide nanoparticles ($Fe_3O_4$ NPs) were successfully entrapped into chitosan surface.

## TOXICITY STUDIES

The BSLT method is used as a simple bioassay to monitor the pharmacological activity and toxicity of samples. The advantages of BSLT are simple, fast, cheap, and requiring relatively few samples. This study was conducted to obtain the iron-oxide modified chitosan/Sm/ranitidine composites as antifungal agent and determine their toxicity from each component, thereby ensuring safe application in drug delivery system. To evaluate the toxicity of the iron-oxide modified chitosan/Sm/ranitidine composites, chitosan, Sm salt, and $Fe_3O_4$ NPs, larvae of *A. salina* were used to determine 50% lethal concentration ($LC_{50}$). The $LC_{50}$ described the amount of a chemical substance inhaled by a test animal that causes death in 50% of the test animals used during a toxicity test study. This value is used to deduce the dose required to show toxic effects in humans. Several function of toxicity tests are (i) to detect the intrinsic toxicity of a substance, target organs, and species sensitivity; (ii) to obtain hazard information after acute exposure to a substance; (3) to obtain initial information that can be used to determine dose levels; and (4) to design a toxicity test.

In this study, chitosan was used to encapsulate the matrix for drug delivery system. The $Fe_3O_4$ NPs had the highest toxicity, with $LC_{50}$ value being 2,355 µg/mL compared to Sm and chitosan with toxicity of 3,255 µg/mL and 5,833 µg/mL, respectively. These results were similar with those obtained by Thanou, Verhoef and Junginger (2001), where chitosan was identified as a non-toxic and biocompatible polymer. Chitosan was used for application in drug delivery system as an absorption enhancer of hydrophilic macromolecular drugs. This was because chitosan could be deprotonated at pH level below 6.5 (Kusrini et al. 2014), increasing the paracellular permeability of peptide drug across mucosal epithelia (Thanou, Verhoef & Junginger 2001). Comparison of toxicity properties of starting material, chitosan/Sm complex, and the iron-oxide modified chitosan/Sm/ranitidine composites is presented in Figure 4.

In this study, toxicity of chitosan was reduced after incorporation with Sm and $Fe_3O_4$ NPs to form composites. The toxicity properties of composites A (3,760 µg/mL), B (3,900 µg/mL), and C (3,324 ppm) were similar to Sm salt (3,255 µg/mL). Furthermore, the toxicity properties of the iron-oxide modified chitosan/Sm/ranitidine composites were similar to the control. Increasing concentration of $Fe_3O_4$ NPs from 5 to 25 mg, changing from composite A to C, the toxicity slightly increased from 3,740 µg/mL to 3,324 µg/mL, as shown in Table 2. Meanwhile, composite A with increasing Sm salt from 250 mg to 350 mg, was relatively unchanged, suggesting that $Sm^{3+}$ ions had no significant influence. The interaction between chitosan and $Sm^{3+}$ ions occurred through amine and hydroxyl groups, with composite B showing the highest composite. Moreover, the BSLT method was only an initial step of toxicity study to investigate the minimum exposure of compound to cells. To observe the clinical application of drug model, there is a need for further evaluation of the impact of composites synthesized in long-term exposure. Based on the results, toxicity of Sm salt and $Fe_3O_4$ NPs are lower, suggesting their application as an antifungal agent. Chelation between $Sm^{3+}$ ion and chitosan also increased antifungal activity of composites, which was closely to Nystatin. Based on the $LC_{50}$ value ranging from 500-5,000 µg/mL, chitosan and the iron-oxide modified chitosan/Sm/ranitidine composites were considered slightly toxic (Mayer et al. 1982).

## ANTIFUNGAL ACTIVITY

Antifungal activity tests were conducted using two methods namely (i) the agar diffusion and (ii) serial dilution method. The agar diffusion method was carried out by preparing samples with different concentrations and diffused into Whatman paper disc. Subsequently, area inhibiting fungi growth was marked and its diameter was measured. Since the iron-oxide modified chitosan/Sm/ranitidine composites were insoluble in water, DMSO was selected as solvent to prevent interfering with the result. All samples were tested at concentrations ranging from 10 to 1,000 µg/mL to determine the optimal concentration of fungal activity. From each culture, 3 dots of Whatman paper disc were measured, calculated, and averaged. Inhibition zone diameter for all samples with concentrations from 1,000 to 10 µg/mL was presented in Figure 5 and Table 3.

Increasing the concentration of materials from 10 to 1,000 µg/mL led to a significant rise in inhibition zone diameter. However, the results showed that varied concentrations of the active component in complexes and composites have no significant effect as an antifungal agent, as shown in Table 3. The inhibition diameter zone of *A. niger* suggested that composite A showed the highest value of 18.33 mm at concentration of 1,000 µg/mL. This value is comparable with tetracycline drug that showed the inhibition zone againts *Escherichia coli* of 18.3 mm (Kusrini et al. 2023b). At the same concentration, Nystatin, as a standard antifungal drug, showed an inhibition zone diameter of 22.67 mm. As for comparison, chitosan-$Tb_2S_3$ nanocomposites prepared at pH 10 had an inhibition zone diameter of 7.15 mm towards *Staphylococcus aureus* (Kusrini et al. 2023a). Additionally, inhibition zone of metal nitrate salt for $Eu(NO_3)_3$, $Tb(NO_3)_3$, and $Zn(NO_3)_2$ against *E. coli* were found to be 9.4, 11.0 and 22.1 mm, respectively (Kusrini et al. 2023b), while these metal nitrate salts also showed the inhibition zone towards *S. aureus* were found to be 14.2, 8.2, and 32 mm, respectively (Kusrini et al. 2023b).

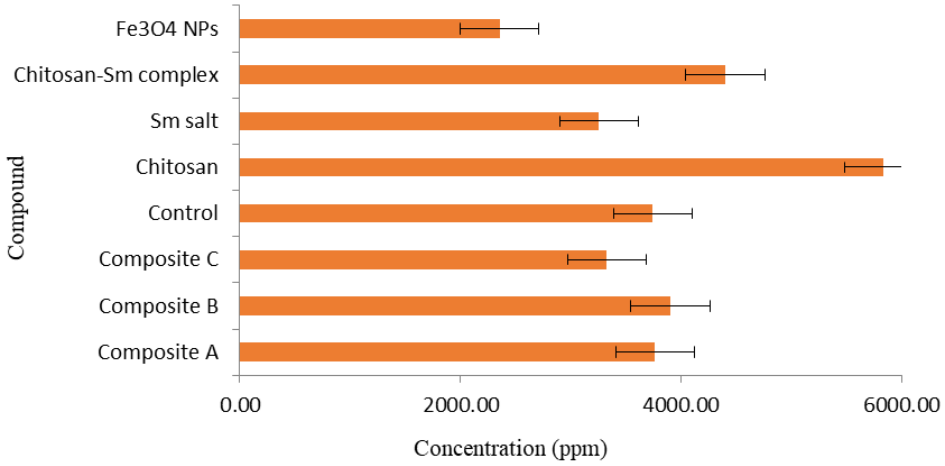


FIGURE 4. Comparison of toxicity properties of starting material, chitosan/Sm complex, and the iron-oxide modified chitosan/Sm/ranitidine composites

TABLE 2. Comparison of toxicity properties of chitosan/Sm complex and the iron-oxide modified chitosan/Sm/ranitidine composites

| Type of compound | Concentration (ppm) |
|---|---|
| Composite A | 3760.83 |
| Composite B | 3900.40 |
| Composite C | 3324.38 |
| Control | 3740.91 |
| Chitosan | 5833.42 |
| $Sm(NO_3)_3.6H_2O$ salt | 3255.44 |
| Chitosan/Sm complex | 4397.90 |
| $Fe_3O_4$ NPs | 2355.03 |

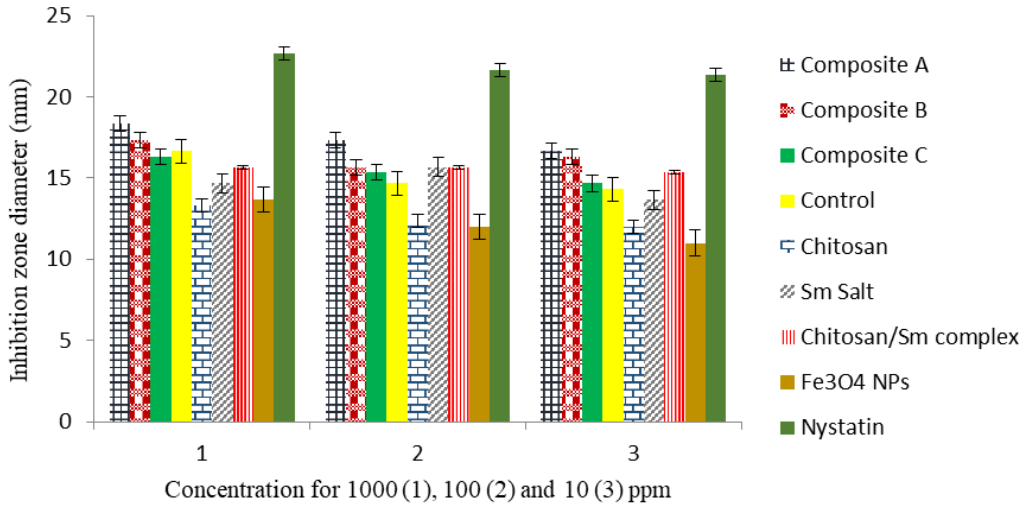


FIGURE 5. Comparison of inhibition zone diameter for composites, chitosan, Sm salt, complex, chitosan/Sm, the iron-oxide, control and Nystatin, where 1 = 1,000 µg/mL, 2 = 100 µg/mL and 3 = 10 µg/mL

TABLE 3. Comparison the effect of concentration of composites A, B, and C, chitosan, chitosan/Sm complex, magnetite, Sm salt, and Nystatin on diameter of the inhibition zone of fungi

| Type of compound | Inhibition Zone diameter (mm) | | |
|---|---|---|---|
| | Concentration (µg/mL) | | |
| | 1,000 | 100 | 10 |
| Composite A | **18.33** | 17.33 | 16.67 |
| Composite B | 17.33 | 15.67 | 16.33 |
| Composite C | 16.33 | 15.33 | 14.67 |
| Control | 16.67 | 14.67 | 14.37 |
| Chitosan/Sm complex | 15.67 | 15.67 | 15.33 |
| Chitosan | 13.33 | 12.33 | 12 |
| $Fe_3O_4$ NPs | 13.67 | 12 | 11 |
| $Sm(NO_3)_3.6H_2O$ salt | 14.67 | 15.67 | 13.67 |
| Nystatin | **22.67** | 21.67 | 21.33 |

The growth inhibition of *A. niger* could be caused by disruption of cell membranes through material composites, which led to the breakdown of cell enzymes (Bhavyasree & Xavier 2020; Sivaraj et al. 2014). These results suggested that the inhibition of *A. niger* mediated by composite A is similar to Nystatin which act as a standard antifungal drug. $Fe_3O_4$ NPs had the lowest inhibition zone diameter of 11 - 13.67 mm, which was similar to CuO/C nanocomposites with a value of 13 mm (Bhavyasree & Xavier 2020).

A serial dilution method was used to determine the minimum fungicidal concentration (MFC) against *A. niger*. This method was considered as the most appropriate approach to predict the concentration, such as number of colonies of organisms, bacteria, or viruses of the unknown samples (Khezripour et al. 2019). The MFC is the lowest concentration of sample that has an inhibitory activity against fungi overnight. As shown in Table 4, MFC values were inspected in concentrations ranging from 1.25 to 10 µg/mL, and microbial growth was observed for $Fe_3O_4$ NPs at 5-1.25 µg/mL. Based on the results, $Fe_3O_4$ NPs had MIC of 10 µg/mL against *A. niger*, which was higher compared to Sm salt and chitosan (5 µg/mL). All composites and chitosan-Sm complex showed MFC of 1.25 µg/mL, suggesting higher antifungal activity as compared with $Fe_3O_4$ NPs. This showed that all composites and chitosan/Sm complex were more potent antifungal activity against *A. niger* strains. The values obtained were comparable to CuO/C nanocomposite with MFC being 1.5 µg/mL (Thanou, Verhoef & Junginger 2001) and the essential oil of *Hypericum triquetrifolium* with MFC being 1.56-25.00 µg/mL (Rouis et al. 2013). In comparison, Nystatin showed the most potent fungistatic activity with no observable microbial growth. *A. niger* is among the most pathogenic microbes, commonly having cell walls based on lipid membranes and high selectivity of materials soluble in lipid. In this study, the lipophilic properties of iron-oxide modified chitosan/Sm/ranitidine composites increased the penetration ability of *A. niger* to the membranes and deactivated enzymes active site or disturbed cell metabolism (Mimouni et al. 2014). The hydroxyl group from chitosan also affected $Na^+$ and $H^+$ ion exchange in cells, thereby disrupting the homeostatic nature of cells. We assumed that other parameters such as viscosity, molar conductivity, and magnetic moment of chitosan/Sm/$Fe_3O_4$ may influence the antimicrobial activity. In this study, the solubility of compounds and selecting of solvent (DMSO) are important and the first priority for preparation of samples and for their antifungal tests.

The antifungal activity of chitosan/Sm complex was comparable to their composites. This finding can be correlated with reactive nature of lanthanides to fungi. The high electropositivity of lanthanides when coordinated with organic ligands facilitated the ability to attack and damage cell walls (Kusrini et al. 2018, 2016). Therefore, the presence of lanthanides in drug delivery system could produce multifunctional drug active substances (Usman et al. 2018).

As shown in Tables 3 and 4, composite A has the highest concentration of $Sm^{3+}$ ion, showing that antifungal activity was the greatest. $Sm^{3+}$ concentration could also be considered to be the most effective in determining antifungal activity of composites. As composites had higher activity compared to starting materials, the chelation of ligands to $Sm^{3+}$ increased the antifungal activity of composites. Additionally, composites with the lowest MFC have inhibitory activity at concentration of 5 µg/mL. Antifungal activity should be affected by other several factors such as sterical, electronic, and pharmacokinetic properties. Moreover, pharmacokinetic theory suggested that chelating lanthanide ions with ranitidine increased

TABLE 4. The MFC of the microparticles of iron-oxide modified chitosan/Sm/ranitidine composites, nystatin, chitosan/Sm complex, and chitosan

| Compounds | Concentration (μg/mL) | | | |
|---|---|---|---|---|
| | 10 | 5 | 2.5 | 1.25 |
| Composite A | - | - | - | + |
| Composite B | - | - | - | + |
| Composite C | - | - | - | + |
| Control | - | - | - | + |
| Chitosan/Sm complex | - | - | - | + |
| Chitosan | - | - | + | + |
| $Fe_3O_4$ NPs | - | + | + | + |
| $Sm(NO_3)_3.6H_2O$ salt | - | - | + | + |
| Nystatin drug | - | - | - | - |

+ = Microbial growth observed, - = Microbial growth inhibited

antifungal activity, as demonstrated in this study. This was attributed to the reduced polarization of $Sm^{3+}$ chelation, where the positive charge was distributed to attached ligand, increasing lipophilic properties of composites (Balasubramanian et al. 2007; Mimouni et al. 2014; Momani et al. 2012; Nishat & Malik 2012).

In this study, by modifying the structure of chitosan core using $Sm^{3+}$ ion, $Fe_3O_4$ NPs, and ranitidine, an improvement of chitosan as an antifungal agent was achieved. On the other hand, the introduction of new active components including $Sm^{3+}$ $Fe_3O_4$ NPs, and ranitidine led to enhanced functionality, serving as a more active antifungal agent. Further investigation and validation are needed to develop new composites based on chitosan, $Sm^{3+}$ ion, $Fe_3O_4$ NPs, and ranitidine as an antifungal agent. Moreover, chitosan is a positively charged polymer amine, allowing attraction to negatively charged ions and pathogens such as in the blood and exudate (Qin, Lia & Guo 2020). The inhibition zone diameter of pure chitosan is 6.8 nm towards *S. aureus*, as reported by Kusrini et al. (2023a, 2023b).

## CONCLUSION

In conclusion, this study showed the procedure to obtain magnetic microparticle composites using chitosan, samarium, magnetic nanoparticles, and ranitidine by the microwave-assisted evaporation method. The iron-oxide modified chitosan/Sm/ranitidine microparticles containing ranitidine with different compositions of chitosan (2,000 - 2,500 mg), samarium (250 - 350 mg), and magnetite nanoparticles (5 - 25 mg) were successfully synthesized, including the evaluation of cytotoxicity and antifungal activity. The results showed that ranitidine as a drug model effectively interacted with $Sm^{3+}$ ions, where $Fe_3O_4$ NPs had the highest toxicity, followed by Sm salt and chitosan. The toxicity value, as represented by 50% lethal concentration ($LC_{50}$) of all starting materials was more than 1,000 μg/mL, and iron-oxide modified chitosan/Sm/ranitidine microparticles showed antifungal activity ranging from 16.33 mm - 18.33 mm, as indicated by the ability of microparticle composites to inhibit *A. niger* with efficiency close to Nystatin at 22.67 mm. All composites and chitosan-Sm complex had MFC of approximately 2.5 μg/mL. In this study, both chitosan and ranitidine acted as ligand to form the chelation with the $Sm^{3+}$ ion. The antifungal activity showed that all iron-oxide modified chitosan/Sm/ranitidine composites had high activity against *A. niger* as compared to individual precursor and ligand when not coordinated into $Sm^{3+}$ in the composites. The modification of the structure of chitosan using $Sm^{3+}$, $Fe_3O_4$ NPs, and ranitidine components improved the physical and chemical properties of chitosan as an antifungal agent. These results could serve as a valuable reference for future studies related to the application of lanthanides in medical or bioimaging fields.

## ACKNOWLEDGMENTS

The authors greatly acknowledge the Universitas Indonesia for providing the *HIBAH PUBLIKASI TERINDEKS INTERNASIONAL (PUTI) Q1 TAHUN ANGGARAN 2024-2025*, NKB-484/UN2.RST/HKP.05.00/2024. Authors thank to Karina Ayuningtyas from Universitas Indonesia for preparing Figure 1.

## REFERENCES

Asrahwi, M.A., Rosman, N.A., Shahri, N.N.M., Santos, J.H., Kusrini, E., Thongratkaew, S., Faungnawakij, K., Hassan, S., Mahadi, A.H. & Usman A. 2023. Solid-state mechanochemical synthesis of chitosan from mud crab (*Scylla serrata*) chitin. *Carbohydrate Research* 534: 108971. https://doi.org/10.1016/j.carres.2023.108971

Balasubramanian, K.P., Karvembu, R., Prabhakaran, R., Chinnusamy, V. & Natarajan, K. 2007. Synthesis, spectral, catalytic and antimicrobial studies of $PPh_3$/$AsPh_3$ complexes of Ru(II) with dibasic tridentate O, N, S donor ligands. *Spectrochimica Acta Part A* 68: 50-54. https://doi.org/10.1016/j.saa.2006.10.049

Bhavyasree, P.G. & Xavier, T.S. 2020. Green synthesis of copper oxide/carbon nanocomposites using the leaf extract of *Adhatoda vasica Nees*, their characterization and antimicrobial activity. *Heliyon* 6: e03323. https://doi.org/10.1016/j.heliyon.2020.e03323

Cota, I., Marturano, V. & Tylkowski, B. 2019. Ln complexes as double faced agents: Study of antibacterial and antifungal activity. *Coordination Chemistry Reviews* 396: 49-71. https://doi.org/10.1016/j.ccr.2019.05.019

Chandra, S. & Agrawal, S. 2014. Spectroscopic characterization of Lanthanoid derived from a hexadentate macrocyclic ligand: Study on antifungal capacity of complexes. *Spectrochimica Acta Part A: Molecular and Biomolecular Spectroscopy* 124: 564-570. https://doi.org/10.1016/j.saa.2014.01.042

Devineni, S.R., Doddaga, S., Donka, R. & Chamarthi, N.R. 2013. $CeCl_3 \cdot 7H_2O$-$SiO_2$: Catalyst promoted microwave assisted neat synthesis, antifungal and antioxidant activities of α-diaminophosphonates. *Chinese Chemical Letters* 24: 759-763. https://doi.org/10.1016/j.cclet.2013.04.037

Hassani, S., Laouini, A., Fessi, H. & Charcosset, C. 2015. Preparation of chitosan–TPP nanoparticles using microengineered membranes - Effect of parameters and encapsulation of tacrine. *Colloids and Surfaces A: Physicochemical and Engineering Aspects* 482: 34-43. https://doi.org/10.1016/j.colsurfa.2015.04.006

Khezripour, A.R., Souri, D., Tavafi, H. & Ghabooli, M. 2019. Serial dilution bioassay for the detection of antibacterial potential of ZnSe quantum dots and their Fourier transform infra-red spectroscopy. *Measurement* 148: 106939. https://doi.org/10.1016/j.measurement.2019.106939

Kusrini, E., Alhamid, M.I., Wulandari, D.A., Fatkhurrahman, M., Shahrin, E.W.E.S., Shahri, N.N.M., Usman, A., Prasetyo, A.B., Sufyan, M., Rahman, A., Nugrahaningtyas, K.D. & Santosa, S.J. 2024. Simultaneous adsorption of multicomponent lanthanide ions on pectin encapsulated zeolite A. *EVERGREEN Joint Journal of Novel Carbon Resource Sciences & Green Asia Strategy* 11(01): 371-378. https://doi.org/10.5109/7172296

Kusrini, E., Safira, A.I., Usman, A., Prasetyanto, E.A., Nugrahaningtyas, K.D., Santosa, S.J. & Wilson, L.D. 2023a. Nanocomposites of terbium sulfide nanoparticles with a chitosan capping agent for antibacterial applications. *Journal of Composites Science* 7: 39. https://doi.org/10.3390/jcs7010039

Kusrini, E., Wilson, L.D., Padmosoedarso, K.M., Mawarni, D.P., Sufyan, M. & Usman, A. 2023b. Synthesis of chitosan capped zinc sulphide nanoparticle composites as an antibacterial agent for liquid handwash disinfectant applications. *Journal of Composites Science* 7: 52. https:// doi.org/10.3390/jcs7020052

Kusrini, E., Sabira, K., Hashim, F., Putra, N., Prasetyanto, E.A., Abdullah, N.A. & Usman, A. 2021. Design, synthesis, and antimicrobial activity of dysprosium-based nanoparticles using contact lenses as carrier against *Acanthamoeba* keratitis. *Acta Ophthalmologica* 99(2): e178-e188. https://doi.org/10.1111/aos.14541

Kusrini, E., Hashim, F., Saleh, M.I., Adnan, R., Usman, A., Zakaria, I.N., Prihandini, W.W., Putra, N. & Prasetyanto, E.A. 2020. Monoclinic cerium(III) picrate tetraethylene glycol complex: Design, synthesis and biological evaluation as anti-amoebic activity against *Acanthamoeba* sp. *Journal of Materials Science* 55: 9795-9811. https://doi.org/10.1007/s10853-020-04793-2

Kusrini, E., Hashim, F., Gunawan, C., Mann, R., Noor Azmi, W.N.N.W.N. & Amin, N.M. 2018. Anti-amoebic activity of acyclic and cyclic-samarium complexes on Acanthamoeba. *Parasitology Research* 117: 1409-1417. https://doi.org/10.1007/s00436-018-5814-x

Kusrini, E., Prassanti, R., Nurjaya, D.M. & Gunawan, C. 2017. Multifunctional microsphere formulation of fluorescent magnetic properties for drug delivery system. *AIP Conference Proceedings* 1817: 030011. https://doi.org/10.1063/1.4976780

Kusrini, E., Hashim, F., Noor Azmi, W.N.N.W., Amin, N.M. & Estuningtyas, A. 2016. A novel antiamoebic agent against *Acanthamoeba* sp. - A causative agent for eye keratitis infection. *Spectrochimica Acta Part A: Molecular and Biomolecular Spectroscopy* 153: 714-721. https://doi.org/10.1016/j.saa.2015.09.021

Kusrini, E., Arbianti, R., Sofyan, N., Abdullah, M.A.A. & Andriani, F. 2014. Modification of chitosan by using samarium for potential use in drug delivery system. *Spectrochimica Acta Part A: Molecular and Biomolecular Spectroscopy* 120: 77-83. http://dx.doi.org/10.1016/j.saa.2013.09.132

Kusrini, E., Sofyan, N., Nurjaya, D.M., Santoso & Tristantini, D. 2013. Removal of heavy metals from aqueous solution by hydroxyapatite/chitosan composite. *Advanced Materials Research* 789: 176-179. https://doi.org/10.4028/www.scientific.net/AMR.789.176

Mayer, B.N., Ferrigni, N.R., Putnam, J.E., Jacobsen, L.B., Nichols, D.E. & McLaughin, J.L. 1982. Brine shrimp: A convenient general bioassay for active plant constituents. *Planta Medica* 45(5): 31-34. https://doi.org/10.1055/s-2007-971236

Mimouni, M., Khardli, F.Z., Warad, I., Ahmad, M., Mubarak, M.S., Sultana, S. & Hadda, T.B. 2014. Antimicrobial activity of naturally occurring antibiotics monensin, lasalocid and their metal complexes. *Journal of Materials Environmental Science* 5(1): 207-214.

Mohanan, K., Kumari, B.S. & Rijulal, G. 2008. Microwave assisted synthesis, spectroscopic, thermal, and antifungal studies of some lanthanide(III) complexes with a heterocyclic bishydrazone. *Journal of Rare Earths* 26: 16-21. https://doi.org/10.1016/S1002-0721(08)60028-9

Momani, W.M.A., Taha, Z.A., Ajlouni, A.A.M., Shaqra, Q.M.A. & Zouby, M.A. 2012. A study of *in vitro* antibacterial activity of lanthanides complexes with a tetradentate Schiff base ligand. *Asian Pacific Journal of Tropical Biomedicine* 3(5): 367-370. https://doi.org/10.1016/S2221-1691(13)60078-7

Nishat, N. & Malik, A. 2012. Synthesis, spectral characterization thermal stability, antimicrobial studies and biodegradation of starch–thiourea based biodegradable polymeric ligand and its coordination complexes with [Mn(II), Co(II), Ni(II), Cu(II), and Zn(II)] metals. *Journal of Saudi Chemical Society* 1319-1332. https://doi.org/10.1016/j.jscs.2012.07.017

Patel, M.P., Patel, R.R. & Patel, J.K. 2010. Chitosan mediated targeted drug delivery system: A review. *Journal of Pharmacy & Pharmaceutical Sciences* 13(3): 536-557. DOI: 10.18433/j3jc7c

Patil, S.K., Naik, V.M., Bilehal, D.C. & Mallur, N.B. 2011. Synthesis, spectral and antimicrobial studies of lanthanide (III) nitrate complexes with terdentate ONO donor hydrazones. *Journal of Experimental Science* 2(7): 15-20.

Peng, H., Liu, G., Dong, X., Wang, J., Yu, W. & Xu, J. 2012. Magnetic, luminescent and core–shell structured $Fe_3O_4$@$YF_3$:$Ce^{3+}$,$Tb^{3+}$ bifunctional nanocomposites. *Powder Technology* 215-216: 242-246. https://doi.org/10.1016/j.powtec.2011.10.006

Qin, Y., Lia, P. & Guo, Z. 2020. Cationic chitosan derivatives as potential antifungals: A review of structural optimization and applications. *Carbohydrate Polymers* 23615: 116002. https://doi.org/10.1016/j.carbpol.2020.116002

Rahdar, A., Aliahmad, M., Samani, M., Majd, M.H. & Susan, M.A.H. 2019. Synthesis and characterization of highly efficacious Fe-doped ceria nanoparticles for cytotoxic and antifungal activity. *Ceramics Internasional* 45: 7950-7955. https://doi.org/10.1016/j.ceramint.2019.01.108

Rosman, N.A., Asrahwi, M.A., Narudin, N.A.H., Sahid, M.S.M., Dewi, R., Shamsuddin, N., Roil Bilad, M., Kusrini, E., Hobley, J. & Usman, A. 2023. Chitin and chitosan: Isolation, deacetylation, and prospective biomedical, cosmetic, and food applications. In *Advanced Materials towards Energy Sustainability.* Boca Raton: CRC Press. pp. 129-150. https://doi.org/10.1201/9781003367819-7

Rouis, Z., Abid, N., Koudja, S., Yangui, T., Elaissi, A., Cioni, P.L., Flamini, G. & Aouni, M. 2013. Evaluation of the cytotoxic effect and antibacterial, antifungal, and antiviral activities of *Hypericum triquetrifolium* Turra essential oils from Tunisia. *BMC Complementary and Alternative Medicine* 13: 24. https://doi.org/10.1186/1472-6882-13-24

Shahri, N.N.M., Taha, H., Hamid, M.H.S.A., Kusrini, E., Lim, J-W., Hobley, J. & Usman, A. 2022. Antimicrobial activity of silver sulfide quantum dots functionalized with highly conjugated Schiff bases in a one-step synthesis. *RSC Advances* 12: 3136-3146. https://doi.org/10.1039/D1RA08296E

Sivaraj, R., Rahman, P.K.S.M., Rajiv, P., Narendhran, S. & Venckatesh, R. 2014. Biosynthesis and characterization of *Acalypha indica* mediated copper oxide nanoparticles and their evaluation of its antimicrobial and anticancer activity. *Spectrochimica Acta, Part A: Molecular and Biomolecular Spectrosc*opy 129: 255-258. https://doi.org/10.1016/j.saa.2014.03.027

Thanou, M., Verhoef, J.C. & Junginger, H.E. 2001. Oral drug absorption enhancement by chitosan and its derivatives. *Advanced Drug Delivery Reviews* 52(2): 117-126. https://doi.org/10.1016/S0169-409X(01)00231-9

Usman, A., Kusrini, E., Wilson L.D., Santos, J.H. & Nur, M. 2024. Chapter 9: Chitosan and chitosan-based nanomaterials in decontamination of pharmaceutical waste. In *Chitosan-Based Hybrid Nanomaterials, Emerging Applications of Chitosan-Based Nanomaterial*, 1st ed., edited by Ali, N., Bilal, M., Khan, A., Nguyen, T.A. Elsevier. pp. 153-180. https://doi.org/10.1016/B978-0-443-21891-0.00009-3

Usman, A., Kusrini, E., Widiantoro, A.B., Hardiya, E., Abdullah, N.A. & Yulizar, Y. 2018. Fabrication of chitosan nanoparticles containing samarium ion potentially applicable for fluorescence detection and energy transfer. *International Journal of Technology* 9(6): 1112-1120. https://doi.org/10.14716/ijtech.v9i6.2576

Wang, W., Xiangpeng, J. & Kezheng, C. 2011. Lanthanide-doped chitosan nanospheres as cell nuclei illuminator and fluorescent nonviral vector for plasmid DNA delivery. *Dalton Transactions* 41: 490-497. https://doi.org/10.1039/C1DT11200G

Wibowo, A., Jatmiko, A., Ananda, M.B., Rachmawati, S.A., Ardy, H., Aimon, A.H. & Iskandar, F. 2021. Facile fabrication of polyelectrolyte complex nanoparticles based on chitosan – poly-2-acrylamido-2-methylpropane sulfonic acid as a potential drug carrier material. *International Journal of Technology* 12(3): 561-570. https://doi.org/10.14716/ijtech.v12i3.4193

Zhao, Y., Qiu, Z. & Huang, J. 2008. Preparation and analysis of $Fe_3O_4$ magnetic nanoparticles used as targeted-drug carriers. *Chinese Journal of Chemical Engineering* 16: 451-455. https://doi.org/10.1016/S1004-9541(08)60104-4

*Corresponding author; email: eny.k@ui.ac.id (EK)

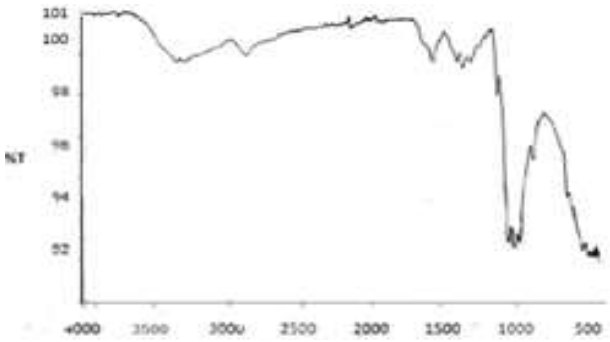


(a)

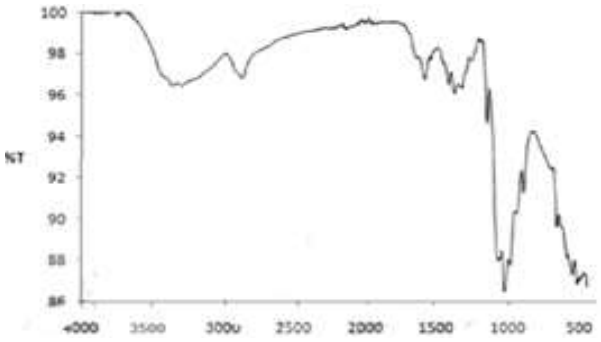


(b)

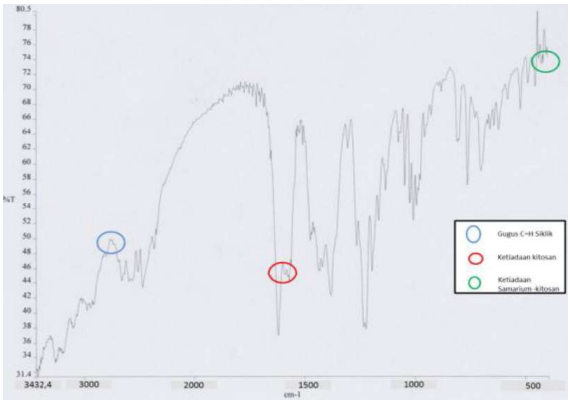


(c)


(d)

FIGURE S1. FTIR Spectra of chitosan (a); chitosan-samarium (b); ranitidine (c); and composite (d)